Fuzzy sliding mode control of a doubly fed induction generator for wind energy conversion

Z. Boudjema, A. Meroufel, Y. Djerriri
Department of Electrical Engineering, University of Sidi
Bel-Abbes, Algeria,
boudjemaa1983@yahoo.fr

E. Bounadja
Department of Electrical Engineering,
University of Chlef, Algeria,
e.bounadja@univ-chlef.dz

Abstract—**In this paper we present a nonlinear control using fuzzy sliding mode for wind energy conversion system based on a doubly-fed induction generator (DFIG) supplied by an AC-AC converter. In the first place, we carried out briefly a study of modeling on the whole system. In order to control the power flowing between the stator of the DFIG and the grid, a proposed control design uses fuzzy logic technique is applied for implementing a fuzzy hitting control law to remove completely the chattering phenomenon on a conventional sliding mode control. The use of this method provides very satisfactory performance for the DFIG control, and the chattering effect is also reduced by the fuzzy mode. The machine is tested in association with a wind turbine. Simulations results are presented and discussed for the whole system.**

Key words — **Doubly fed induction generator, matrix converter, fuzzy sliding mode controller, wind energy.**

I. INTRODUCTION

Wind energy is the most promising renewable source of electrical power generation for the future. Many countries promote the wind power technology through various national programs and market incentives. Wind energy technology has evolved rapidly over the past three decades with increasing rotor diameters and the use of sophisticated power electronics to allow operation at variable speed [1].

Doubly fed induction generator (DFIG) is one of the most popular variable speed wind turbines in use nowadays. It is normally fed by a voltage source inverter. However, currently the three phase matrix converters have received considerable attention because they may become a good alternative to voltage-source inverter Pulse Width-Modulation (PWM) topology. This is because the matrix converter provides bi-directional power flow, nearly sinusoidal input/output waveforms, and a controllable input power factor. Furthermore, the matrix converter allows a compact design due to the lack of dc-link capacitors for energy storage. Consequently, in this work, a three-phase matrix converter is used to drive the DFIG.

A lot of works have been presented with diverse control diagrams of DFIG. These control diagrams are usually based on vector control notion with conventional PI controllers as proposed by Pena et al. in [2]. The similar conventional controllers are also used to realize control techniques of DFIG

when grid faults appear like unbalanced voltages [3,4] and voltage dips [5]. It has also been shown in [6,7] that glimmer problems could be resolved with suitable control strategies. Many of these works prove that stator reactive power control can be an adapted solution to these diverse problems.

In recent years, the sliding mode control (SMC) methodology has been widely used for robust control of nonlinear systems. Sliding mode control, based on the theory of variable structure systems (VSS), has attracted a lot of research on control systems for the last two decades. It achieves robust control by adding a discontinuous control signal across the sliding surface, satisfying the sliding condition. Nevertheless, this type of control has an essential disadvantage, which is the chattering phenomenon caused by the discontinuous control action. To treat these difficulties, several modifications to the original sliding control law have been proposed, the most popular being the boundary layer approach [8].

Fuzzy logic is a technology based on engineering experience and observations. In fuzzy logic, an exact mathematical model is not necessary because linguistic variables are used to define system behavior rapidly.

One way to improve sliding mode controller performance is to combine it with fuzzy logic to form a fuzzy sliding mode controller (FSMC). The design of a sliding mode controller incorporating fuzzy control helps in achieving reduced chattering, simple rule base, and robustness against disturbances and nonlinearities.

This work is organized as follows. We briefly review the modeling of the device studied in section 2. In section 3 we present the field oriented control of the DFIG. Section 4 provides the detail of the SMC technique and its application to the DFIG control. In section 5 we introduce the FSMC to the DFIG control and discuss its benefits. The effectiveness of the proposed method verified by simulation is presented in section 6. Finally, the main conclusions of the work are drawn.

II. SYSTEM MODELING

A. Wind turbine model

For a horizontal axis wind turbine, the mechanical power captured from the wind is given by:

$$P_t = \frac{1}{2} C_P(\lambda, \beta) R^2 \rho\, v^3 \qquad (1)$$

Where, R is the radius of the turbine (m), ρ is the air density (kg/m^3), v is the wind speed (m/s), and C_P is the power coefficient which is a function of both tip speed ratio λ, and blade pitch angle β (deg). In this work, the C_P equation is approximated using a non-linear function according to [9].

$$C_P = (0.5 - 0.167)(\beta - 2)\sin\left[\frac{\pi(\lambda + 0.1)}{18.5 - 0.3(\beta - 2)}\right] - 0.0018(\lambda - 3)(\beta - 2) \qquad (2)$$

The tip speed ratio is given by:

$$\lambda = \frac{\Omega_t R}{v} \qquad (3)$$

Where Ω_t is the angular velocity of Wind Turbine.

B. The matrix converter model

The matrix converter performs the power conversion directly from AC to AC without any intermediate dc link. It is very simple in structure and has powerful controllability. The converter consists of a matrix of bi-directional switches linking two independent three-phase systems. Each output line is linked to each input line via a bi-directional switch. Fig. 1 shows the basic diagram of a matrix converter.

The switching function of a switch S_{mn} in Fig. 1 is given by :

$$S_{mn} = \begin{cases} 1 & S_{mn} \text{ closed} \\ 0 & S_{mn} \text{ open} \end{cases} \quad m \in \{A, B, C\}, n \in \{a, b, c\} \quad (4)$$

The mathematical expression that represents the operation of the matrix converter in Fig. 1 can be written as :

$$\begin{bmatrix} V_a \\ V_b \\ V_c \end{bmatrix} = \begin{bmatrix} S_{Aa} & S_{Ab} & S_{Ac} \\ S_{Ba} & S_{Bb} & S_{Bc} \\ S_{Ca} & S_{Cb} & S_{Cc} \end{bmatrix} \cdot \begin{bmatrix} V_A \\ V_B \\ V_C \end{bmatrix} \qquad (5)$$

$$\begin{bmatrix} i_A \\ i_B \\ i_C \end{bmatrix} = \begin{bmatrix} S_{Aa} & S_{Ba} & S_{Ca} \\ S_{Ab} & S_{Bb} & S_{Cb} \\ S_{Ac} & S_{Bc} & S_{Cc} \end{bmatrix}^T \cdot \begin{bmatrix} i_a \\ i_b \\ i_c \end{bmatrix} \qquad (6)$$

To determine the behavior of the matrix converter at output frequencies well below the switching frequency, a modulation duty cycle can be defined for each switch.

The input/output relationships of voltages and currents are related to the states of the nine switches and can be expressed as follows :

$$\begin{bmatrix} V_a \\ V_b \\ V_c \end{bmatrix} = \begin{bmatrix} k_{Aa} & k_{Ab} & k_{Ac} \\ k_{Ba} & k_{Bb} & k_{Bc} \\ k_{Ca} & k_{Cb} & k_{Cc} \end{bmatrix} \cdot \begin{bmatrix} V_A \\ V_B \\ V_C \end{bmatrix} \qquad (7)$$

$$\begin{bmatrix} i_A \\ i_B \\ i_C \end{bmatrix} = \begin{bmatrix} k_{Aa} & k_{Ba} & k_{Ca} \\ k_{Ab} & k_{Bb} & k_{Cb} \\ k_{Ac} & k_{Bc} & k_{Cc} \end{bmatrix}^T \cdot \begin{bmatrix} i_a \\ i_b \\ i_c \end{bmatrix} \qquad (8)$$

With :

$$0 \le k_{mn} \le 1, \quad m = A, B, C, \quad n = a, b, c \qquad (9)$$

The variables k_{mn} are the duty cycles of the nine switches S_{mn} and can be represented by the duty-cycle matrix k. In order to prevent a short circuit on the input side and ensure uninterrupted load current flow, these duty cycles must satisfy the three following constraint conditions :

$$k_{Aa} + k_{Ab} + k_{Ac} = 1 \qquad (10)$$
$$k_{Ba} + k_{Bb} + k_{Bc} = 1 \qquad (11)$$
$$k_{Ca} + k_{Cb} + k_{Cc} = 1 \qquad (12)$$

The high-frequency synthesis technique introduced by Venturini (1980) and Alesina and Venturini (1988), allows a control of the S_{mn} switches so that the low frequency parts of the synthesized output voltages (V_a, V_b and V_c) and the input currents (i_A, i_B and i_C) are purely sinusoidal with the prescribed values of the output frequency, the input frequency, the displacement factor and the input amplitude.

The output voltage is given by :

$$\begin{bmatrix} V_a \\ V_b \\ V_c \end{bmatrix} = \begin{bmatrix} 1 + 2\delta\cos\alpha & 1 + 2\delta\cos(\alpha - \frac{2\pi}{3}) & 1 + 2\delta\cos(\alpha - \frac{4\pi}{3}) \\ 1 + 2\delta\cos(\alpha - \frac{4\pi}{3}) & 1 + 2\delta\cos\alpha & 1 + 2\delta\cos(\alpha - \frac{2\pi}{3}) \\ 1 + 2\delta\cos(\alpha - \frac{2\pi}{3}) & 1 + 2\delta\cos(\alpha - \frac{4\pi}{3}) & 1 + 2\delta\cos\alpha \end{bmatrix} \begin{bmatrix} V_A \\ V_B \\ V_C \end{bmatrix} \qquad (13)$$

Where : $\begin{cases} \alpha = \omega_m + \theta \\ \omega_m = \omega_{output} - \omega_{input} \end{cases}$
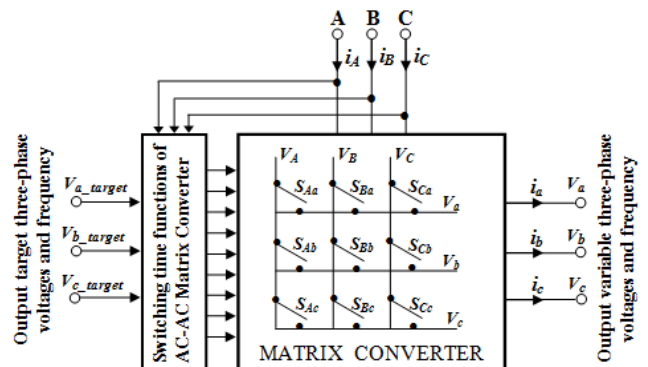

Fig. 1. Schematic representation of the matrix converter.

The running matrix converter with Venturini algorithm generates at the output a three-phases sinusoidal voltages system having in that order pulsation ω_m, a phase angle θ and amplitude $\delta.V_s$ ($0 < \delta < 0.866$ with modulation of the neural) [10].

C. The DFIG Model

The application of Concordia and Park's transformation to the three-phase model of the DFIG permits to write the dynamic voltages and fluxes equations in an arbitrary *d–q* reference frame :

$$\begin{cases} V_{ds} = R_s I_{ds} + \dfrac{d}{dt}\psi_{ds} - \omega_s\psi_{qs} \\[2mm] V_{qs} = R_s I_{qs} + \dfrac{d}{dt}\psi_{qs} + \omega_s\psi_{ds} \\[2mm] V_{dr} = R_r I_{dr} + \dfrac{d}{dt}\psi_{dr} - \omega_r\psi_{qr} \\[2mm] V_{qr} = R_r I_{qr} + \dfrac{d}{dt}\psi_{qr} + \omega_r\psi_{dr} \end{cases} , \begin{cases} \psi_{ds} = L_s I_{ds} + M I_{dr} \\[2mm] \psi_{qs} = L_s I_{qs} + M I_{qr} \\[2mm] \psi_{dr} = L_r I_{dr} + M I_{ds} \\[2mm] \psi_{qr} = L_r I_{qr} + M I_{qs} \end{cases} \quad (14)$$

V_{sd}, V_{sa}, V_{rd} and V_{ra} are respectively the direct and quadrature stator and rotor voltages, I_{sd}, I_{sa}, I_{rd} and I_{ra} are the direct and quadrature stator and rotor currents, R_s and R_r are respectively the resistances of the rotor and stator windings, L_s, L_r and M are respectively the inductance own stator, rotor, and the mutual inductance between two coils. ψ_{sd}, ψ_{sa}, ψ_{rd} and ψ_{ra} are respectively the direct and quadrature components of stator and rotor fluxes.

The stator and rotor angular velocities are linked by the following relation: $\omega_s = \omega + \omega_r$, where ω_s is the electrical pulsation of the stator and ω_r is the rotor one, ω is the mechanical pulsation of the DFIG.

This electrical model is completed by the mechanical equation :

$$C_{em} = C_r + J\frac{d\Omega}{dt} + f\Omega \qquad (15)$$

Where the electromagnetic torque C_{em} can be written as a function of stator fluxes and rotor currents :

$$C_{em} = -p\frac{M}{L_s}(\psi_{qs}I_{dr} - \psi_{ds}I_{qr}) \qquad (16)$$

With, C_r is the resisting torque, Ω is the mechanical speed of the DFIG, J is the inertia, f is the viscous friction and p is the number of the pairs of poles

III.   FIELD ORIENTED CONTROL OF THE DFIG

In order to easily control the production of electricity by the wind turbine, we will carry out an independent control of active and reactive powers by orientation of the stator flux.

By choosing a reference frame linked to the stator flux, rotor currents will be related directly to the stator active and reactive power. An adapted control of these currents will thus

permit to control the power exchanged between the stator and the grid. If the stator flux is linked to the d-axis of the frame we have :

$$\psi_{ds} = \psi_s \quad \text{and} \quad \psi_{qs} = 0 \qquad (17)$$

and the electromagnetic torque can then be expressed as follows :

$$C_{em} = -p\frac{M}{L_s}I_{qr}\psi_{ds} \qquad (18)$$

By substituting Eq.18 in Eq.15, the following rotor flux equations are obtained :

$$\begin{cases} \psi_s = L_s I_{ds} + M I_{dr} \\[2mm] 0 = L_s I_{qs} + M I_{qr} \end{cases} \qquad (19)$$

In addition, the stator voltage equations are reduced to :

$$\begin{cases} V_{ds} = R_s I_{ds} + \dfrac{d}{dt}\psi_s \\[2mm] V_{qs} = R_s I_{qs} + \omega_s\psi_s \end{cases} \qquad (20)$$

By supposing that the electrical supply network is stable, having for simple voltage V_s, which led to a stator flux ψ_s constant. This consideration associated with Eq.19 shows that the electromagnetic torque only depends on the *q*-axis rotor current component. With these assumptions, the new stator voltage expressions can be written as follows :

$$\begin{cases} V_{ds} = R_s I_{ds} \\[2mm] V_{qs} = R_s I_{qs} + \omega_s\psi_s \end{cases} \qquad (21)$$

Using Eq.20, a relation between the stator and rotor currents can be established :

$$\begin{cases} I_{ds} = -\dfrac{M}{L_s}I_{dr} + \dfrac{\psi_s}{L_s} \\[2mm] I_{qs} = -\dfrac{M}{L_s}I_{qr} \end{cases} \qquad (22)$$

The stator active and reactive powers are written :

$$\begin{cases} P_s = V_{ds}I_{ds} + V_{qs}I_{qs} \\[2mm] Q_s = V_{qs}I_{ds} - V_{ds}I_{qs} \end{cases} \qquad (23)$$

By using Eqs.14, 15, 12 and 23, the statoric active and reactive power, the rotoric fluxes and voltages can be written versus rotoric currents as :

$$\begin{cases} P_s = \dfrac{\omega_s \psi_s M}{L_s} I_{qr} \\[4mm] Q_s = -\dfrac{\omega_s \psi_s M}{L_s} I_{dr} + \dfrac{\omega_s \psi_s^{\,2}}{L_s} \end{cases} \tag{24}$$

$$\begin{cases} \psi_{dr} = (L_r - \dfrac{M^2}{L_s}) I_{dr} + \dfrac{M \psi_s}{L_s} \\[4mm] \psi_{qr} = (L_r - \dfrac{M^2}{L_s}) I_{qr} \end{cases} \tag{25}$$

$$\begin{cases} V_{dr} = R_r I_{dr} + (L_r - \dfrac{M^2}{L_s})\dfrac{dI_{dr}}{dt} - g\omega_s (L_r - \dfrac{M^2}{L_s}) I_{qr} \\[4mm] V_{qr} = R_r I_{qr} + (L_r - \dfrac{M^2}{L_s})\dfrac{dI_{qr}}{dt} + g\omega_s (L_r - \dfrac{M^2}{L_s}) I_{dr} + g\omega_s \dfrac{M \psi_s}{L_s} \end{cases} \tag{26}$$

In steady state, the second derivative terms of the two equations in 27 are nil. We can thus write :

$$\begin{cases} V_{dr} = R_r I_{dr} - g\omega_s (L_r - \dfrac{M^2}{L_s}) I_{qr} \\[4mm] V_{qr} = R_r I_{qr} + g\omega_s (L_r - \dfrac{M^2}{L_s}) I_{dr} + g\omega_s \dfrac{M \psi_s}{L_s} \end{cases} \tag{27}$$

The third term, which constitutes cross-coupling terms, can be neglected because of their small influence. These terms can be compensated by an adequate synthesis of the regulators in the control loops.

IV. SLIDING MODE CONTROL

The sliding mode technique is developed from variable structure control to solve the disadvantages of other designs of nonlinear control systems. The sliding mode is a technique to adjust feedback by previously defining a surface. The system which is controlled will be forced to that surface, then the behavior of the system slides to the desired equilibrium point.

The main feature of this control is that we only need to drive the error to a "switching surface". When the system is in "sliding mode", the system behavior is not affected by any modeling uncertainties and/or disturbances. The design of the control system will be demonstrated for a nonlinear system presented in the canonical form [11] :

$$\dot{x} = f(x,t) + B(x,t) U(x,t), \; x \in R^n, \; U \in R^m, \; ran(B(x,t)) = m \tag{28}$$

with control in the sliding mode, the goal is to keep the system motion on the manifold S, which is defined as :

$$S = \{x : e(x, t)=0\} \tag{29}$$
$$e = x^d - x \tag{30}$$

Here e is the tracking error vector, x^d is the desired state, x is the state vector. The control input U has to guarantee that the motion of the system described in (28) is restricted to belong to the manifold S in the state space. The sliding mode control should be chosen such that the candidate Lyapunov function satisfies the Lyapunov stability criteria:

$$\vartheta = \frac{1}{2} S(x)^2, \tag{31}$$

$$\dot{\vartheta} = S(x)\dot{S}(x). \tag{32}$$

This can be assured for :

$$\dot{\vartheta} = -\eta \left| S(x) \right| \tag{33}$$

Here η is strictly positive. Essentially, equation (31) states that the squared "distance" to the surface, measured by $e(x)^2$, decreases along all system trajectories. Therefore (32), (33) satisfy the Lyapunov condition. With selected Lyapunov function the stability of the whole control system is guaranteed. The control function will satisfy reaching conditions in the following form :

$$U^{com} = U^{eq} + U^n \tag{34}$$

Here U^{com} is the control vector, U^{eq} is the equivalent control vector, U^n is the correction factor and must be calculated so that the stability conditions for the selected control are satisfied.

$$U^n = K \, \mathrm{sat}(S(x)) \tag{35}$$

Where $\mathrm{sat}(S(x))$ is the proposed saturation function, K is the controller gain.

In this paper we propose the Slotine method [12]:

$$S(X) = \left(\frac{d}{dt} + \xi \right)^{n-1} e \tag{36}$$

Here, e is the tracking error vector, ξ is a positive coefficient and n is the relative degree.

A. Application to the DFIG control

In our study, we choose the error between the measured and references stator powers as sliding mode surfaces, so we can write the following expression:

$$\begin{cases} S_d = P_{S-ref} - P_S \\ S_q = Q_{S-ref} - Q_S \end{cases} \tag{37}$$

The first order derivate of (37), gives :

$$\begin{cases} \dot{S}_d = \dot{P}_{S-ref} - \dot{P}_S \\ \dot{S}_q = \dot{Q}_{S-ref} - \dot{Q}_S \end{cases} \tag{38}$$

Replacing the powers in (38) by their expressions given in (24), one obtains:

$$\begin{cases} \dot{S}_1 = \dot{P}_{S-ref} - \dfrac{\omega_s \psi_s M}{L_s} \dot{I}_{qr} \\ \dot{S}_2 = \dot{Q}_{S-ref} + \dfrac{\omega_s \psi_s M}{L_s} \dot{I}_{dr} - \dfrac{\omega_s \psi_s^{\,2}}{L_s} \end{cases} \qquad (39)$$

V_{dr} and V_{qr} will be the two components of the control vector used to constraint the system to converge to $S_{dq}=0$. The control vector V_{dqeq} is obtained by imposing $\dot{S}_{dq}=0$ so the equivalent control components are given by the following relation :

$$V_{eqdq} = \begin{bmatrix} -\dfrac{L_s \left(L_r - \dfrac{M^2}{L_s} \right)}{\omega_s \psi_s M} \dot{Q}_s^* + R_r I_{dr} - \left(L_r - \dfrac{M^2}{L_s} \right) g\omega_s I_{qr} + \dfrac{\left(L_r - \dfrac{M^2}{L_s} \right)\psi_s}{M} \\ \dfrac{L_s}{\omega_s \psi_s M} \dot{P}_s^* + R_r I_{qr} - \left(L_r - \dfrac{M^2}{L_s} \right) g\omega_s I_{dr} + \dfrac{g\omega_s \psi_s M}{L_s} \end{bmatrix} \qquad (40)$$

To obtain good performances, dynamic and commutations around the surfaces, the control vector is imposed as follows :

$$V_{dq} = V_{eqdq} + \mathrm{K} \cdot sat\left(S_{dq}\right) \qquad (41)$$

The sliding mode will exist only if the following condition is met :

$$S \cdot \dot{S} < 0 \qquad (42)$$

V.   FUZZY SLIDING MODE CONTROL

The disadvantage of sliding mode controllers is that the discontinuous control signal produces chattering. In order to eliminate the chattering phenomenon, we propose to use the fuzzy sliding mode control.

The fuzzy sliding mode controller (FSMC) is a modification of the sliding mode controller, where the switching controller term sat($S(x)$), has been replaced by a fuzzy control input as given below [13].

$$U^{com} = U^{eq} + U^{Fuzzy} \qquad (43)$$

The proposed fuzzy sliding mode control, which is designed to control the active and reactive power of the DFIG is shown in Fig. 2.

For the two proposed fuzzy sliding mode controllers in Fig. 2, the universes of discourses are first partitioned into the seven linguistic variables NB, NM, NS, EZ, PS, PM, PB, triangular membership functions are chosen to represent the linguistic variables and fuzzy singletons for the outputs are used. The fuzzy rules that produce these control actions are reported in Table 1.

We use the following designations for membership functions:

- NB: Negative Big,   - NM: Negative Middle,

- NS: Negative Small,   - EZ: Equal Zero,
- PS: Positive Small,   - PM: Positive Middle,
- PB: Positive Big.
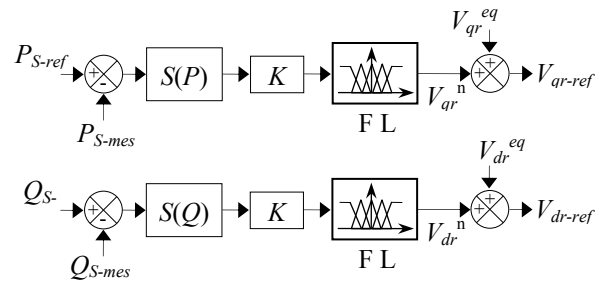
These choices are described in Fig. 3.

Fig. 2. Bloc diagram of the DFIG control with FSMC.

TABLE I.
MATRIX OF INFERENCE

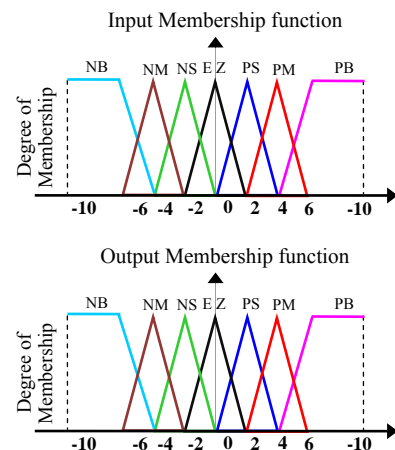| ΔE \ E	NB	NM	NS	EZ	PS	PM	PB
NB	NB	NB	NB	NB	NM	NS	EZ
NM	NB	NB	NB	NM	NS	EZ	PS
NS	NB	NB	NM	NS	EZ	PS	PM
EZ	NB	NM	NS	EZ	PS	PM	PB
PS	NM	NS	EZ	PS	PM	PB	PB
PM	NS	EZ	PS	PM	PB	PB	PB
PB	EZ	PS	PM	PB	PB	PB	PB

Fig. 3. Fuzzy sets and its memberships functions.

VI.   SIMULATION RESULTS AND DISCUSSIONS

In the objective to appraise the performances of the FSMC controller, simulation tests are realized with a 1.5 MW generator coupled to a 398V/50Hz grid. The machine's parameters are given next in appendix. Simulation of the whole system has been realized using Matlab Simulink.

Fig. 5 shows the harmonic spectrum of one phase stator current of the DFIG obtained using Fast Fourier Transform (FFT) technique for SMC controller and FSMC one respectively. It can be clear observed that the total harmonic distortion (THD) is reduced for FSMC controller (THD = 2.85%) when compared to the SMC one (THD = 3.05%).

Therefore we can conclude that the proposed controller is superior to SMC in eliminating chattering phenomena.

Fig. 6 shows the simulation results of the whole system given by the bloc diagram in Fig. 4. This diagram presents a DFIG model associated with a wind turbine which is controlled with MPPT (Maximum Power Point Tracking) strategy. As it's shown by these results, for a variable wind speed the stator active power produced by the DFIG is controlled according to the MPPT strategy and is limited to 1.5 MW which represents the nominal power of the DFIG while the stator reactive power is maintained to zero. In addition, it can be notice that the direct and quadrature rotor current take the same forms like the stator reactive and active power respectively, this reflects Eq. 24. In another side, Fig. 6 shows too that the currents obtained at the DFIG stator have sinusoidal form, which implies a clean energy without harmonics provided by the DFIG.

VII.   CONCLUSION

The modeling, the control and the simulation of an electrical power electromechanical conversion system based on a doubly fed induction generator (DFIG) connected directly to the grid by the stator and fed by a matrix converter on the rotor side has been presented in this paper. Our objective was the implementation of a fuzzy sliding mode control method of active and reactive powers generated by the stator side of the DFIG, in order to ensure of the high performance and a better execution of the DFIG, and to make the system insensible with the external disturbances and the parametric variations. In the first step, we started with a study of modeling on the whole system. In second step, we adopted a vector control strategy in order to control statoric active and reactive power exchanged between the DFIG and the grid. In third step, the description of the classical sliding mode controller (SMC) is presented in detail. Then, the fuzzy logic control is used to mimic the hitting control law to remove the chattering. Compared with the conventional sliding mode controller, the fuzzy sliding mode control system results in robust control performance without chattering. The chattering free improved performance of the FSMC makes it superior to conventional SMC, and establishes its suitability for the system drive.
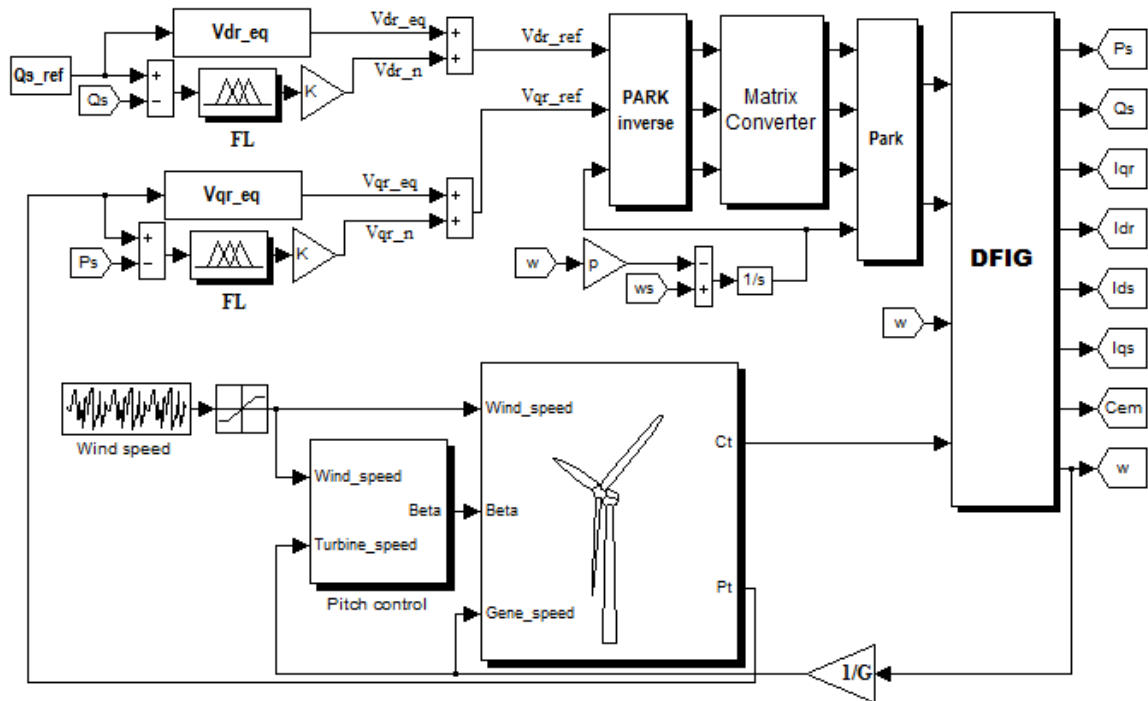

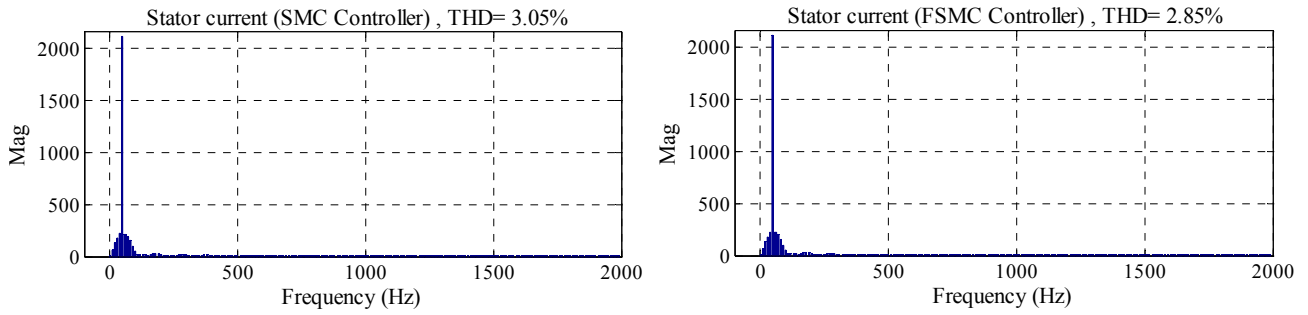Fig. 4. Bloc diagram of the whole device studied under simulation/matlab.

Fig. 5. Spectrum harmonic of one phase stator current for SMC and FSMC controllers.
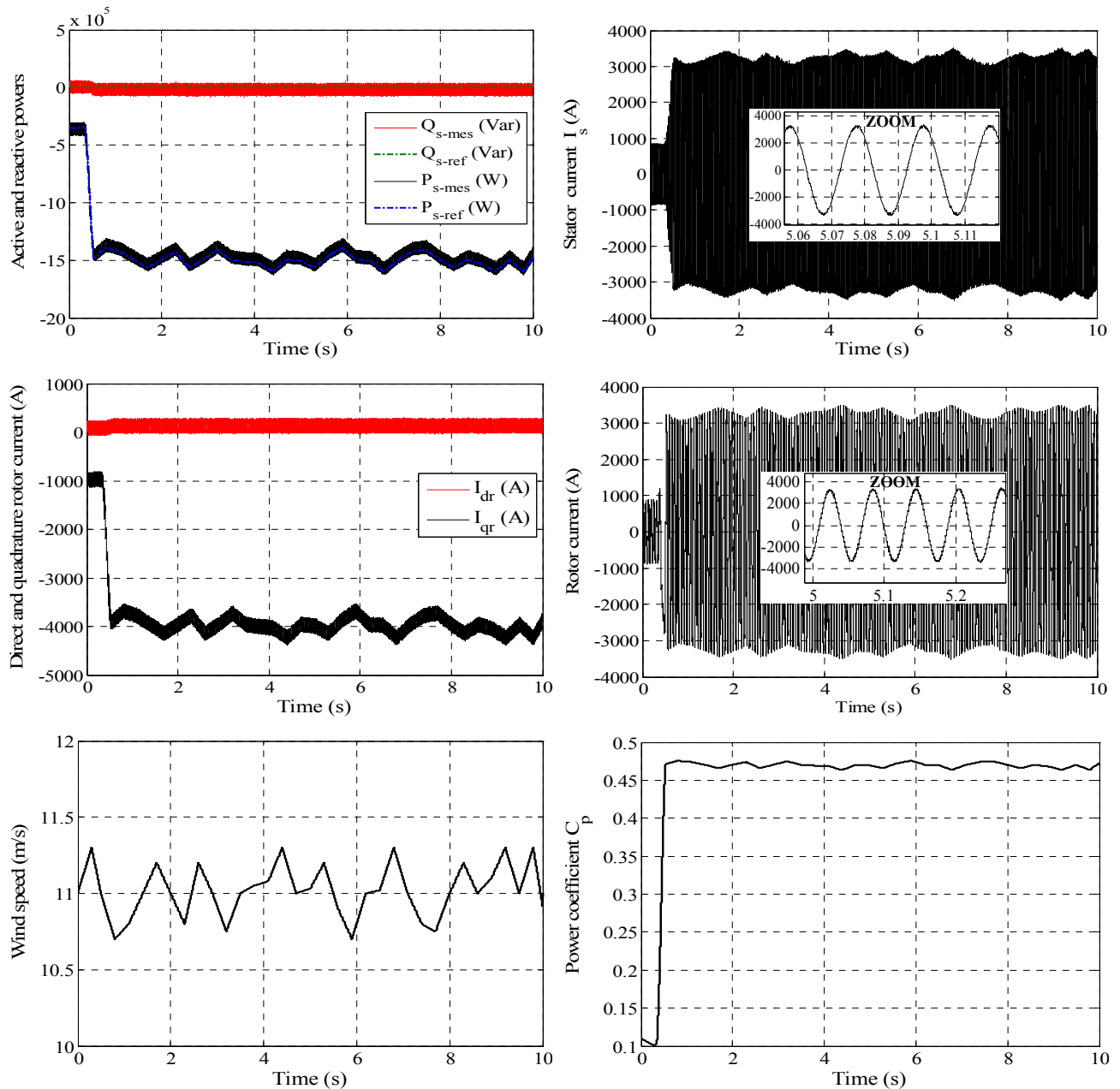

Fig. 6. Whole system simulation results: statoric active and reactive power, DFIG's stator and rotor currents, wind's speed and power coefficient.

APPENDIX

TABLE II.
WIND TURBINE SYSTEM PARAMETERS.

Parameters	Value	IS-Unit
Nominal power	1.5	MW
Turbine radius	35.25	m
Gearbox gain	90	
Stator voltage	398/690	V
Stator frequency	50	Hz
Number of pairs poles	2	
Nominal speed	150	rad/s
Stator resistance	0.012	Ω
Rotor resistance	0.021	Ω
Stator inductance	0.0137	H
Rotor inductance	0.0136	H
Mutual inductance	0.0135	H
Inertia	1000	$Kg.m^2$

REFERENCES

[1] O. Anaya-Lara, N. Jenkins, J. Ekanayake, P. Cartwright, M. Hughes, "Wind Energy Generation," *In : Wiley*, 2009.

[2] R. Pena, J. C. Clare, G. M. Asher, "A doubly fed induction generator using back to back converters supplying an isolated load from a variable speed wind turbine," *In: IEE Proceeding on Electrical Power Applications 143*, September 5, 1996.

[3] M. A. Poller, "Doubly-fed induction machine models for stability assessment of wind farms," *In: Power Tech Conference Proceedings, 2003, IEEE, Bologna*, vol. 3, 23–26, June 2003.

[4] T. Brekken, N. Mohan, "A novel doubly-fed induction wind generator control scheme for reactive power control and torque pulsation compensation under unbalanced grid voltage conditions," *In: IEEE 34th Annual Power Electronics Specialist Conference,* 2003, PESC'03, 15-19 June 2003, vol. 2, pp. 760-764.

[5] T. K. A. Brekken, N. Mohan, "Control of a doubly fed induction wind generator under unbalanced grid voltage conditions," *In: IEEE Transaction on Energy Conversion*, 22 March, 2007 129–135.

[6] J. Lopez, P. Sanchis, X. Roboam, L. Marroyo, "Dynamic behavior of the doubly fed induction generator during three-phase voltage dips," *In: IEEE Transaction on Energy Conversion*, 22 September, 2007, 709–717.

[7] T. Sun, Z. Chen, F. Blaabjerg, "Flicker study on variable speed wind turbines with doubly fed induction generators," *IEEE Transactions on Energy Conversion*, 20 December, 2005, 896–905.

[8] M. A. A. Morsy, M. Said, A. Moteleb, H. Dorrah, "Design and Implementation of Fuzzy Sliding Mode Controller for Switched Reluctance Motor," *Proceedings of the International MultiConference of Engineers and Computer Scientists,* Vol. 2, IMECS, Hong Kong, 19-21 March 2008.

[9] E. S. Abdin, W. Xu, "Control design and Dynamic Performance Analysis of a Wind Turbine Induction Generator Unit," *IEEE Trans. On Energy conversion,* Vol.15, No1, March 2000.

[10] M. Venturini, "A new sine wave in sine wave out conversion technique which eliminates reactive elements," *In: Proc Powercon 7, San Diego*, CA, pp E3-1, E3-15, 27-24 March 1980.

[11] Z. Yan, C. Jin, V. I. Utkin, "Sensorless Sliding-Mode Control of Induction Motors," *IEEE Trans. Ind. electronic.* 47 No. 6, 1286–1297, December 2000.

[12] M. O. Mahmoudi, N. Madani, M. F. Benkhoris, and F. Boudjema, "Cascade sliding mode control of field oriented induction machine drive," *The European Physical Journal. Applied Physics*, pp217-225, 1999.

[13] L. K. Wong, F. H. F. Leung, P. K. S. Tam, "A fuzzy sliding controller for non linear systems," *IEEE Trans. Ind. electronic*, Vol. 48, no.1, pp.32-37, February 2001.

Zinelaabidine Boudjema (correspondent author) was born in Chlef (Algeria) 1983. He is a PhD student in the Department of Electrical Engineering at the university of Djillali liabes, Sidi bel-abbes, Algeria. He received a M.A. degree in Electrical Engineering from ENSET of Oran (Algeria). His research activities include the study and application of robust control in the wind-solar power systems. (E-mail: boudjemaa1983@yahoo.fr).

Abdelkader Meroufel was born in Sidi Bel-Abbes (Algeria) 1954. He received the M.A. degree from the University of Sciences and Technology (USTO), Oran, Algeria and the doctorate degree from the Electrical Engineering Department of University of Sidi Bel-Abbes. Since 1992, he is teaching at the university of Djillali liabes, Sidi bel-abbes, Algeria. His research interests are robust control of electrical machines, control of electric drives. (E-mail: ameroufel@yahoo.fr).

Youcef Djerriri was born in Sidi Bel-Abbes (Algeria) 1984. He is a PhD student in the Department of Electrical Engineering at the university of Djillali liabes, Sidi bel-abbes, Algeria. He received a M.A. degree in Electrical Engineering from the university of Sidi bel-abbes. His research interests are in the field of advanced and intelligent control methods of AC drives associated with power electronic converters for the wind energy conversion systems applications. (E-mail: djeriri_youcef@yahoo.fr).

Elhadj Bounadja was born in Chlef (Algeria) 1970. He is with the Department of Electrical Engineering, University of Hassiba Benbouali, Chlef, Algeria. He received a M.A. degree in Electrical Engineering from the University of Chlef. His research activities include the study and application of intelligent and robust control in the wind power systems. (E-mail: e.bounadja@univ-chlef.dz).